



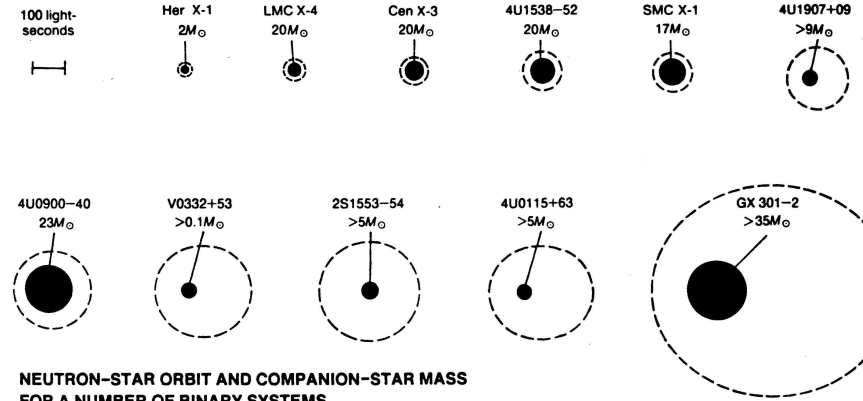
5-1

Accretion onto Magnetized Neutron Stars



5-3

High Mass X-ray Binaries



NEUTRON-STAR ORBIT AND COMPANION-STAR MASS
FOR A NUMBER OF BINARY SYSTEMS

Charles & Seward (1995, Fig. 7.7a)

High-Mass X-ray Binaries: Donor star has early spectral type (O, B), and mass $M \gtrsim 6 M_{\odot}$, wind accretors, Roche lobe overflow, or Be accretion.



Magnetic Fields

5-2

Neutron stars are expected to have strong B -fields!

Neutron stars are formed in supernova explosions.

One of the conserved quantities is the magnetic flux,

$$\Phi = 4\pi R^2 B \implies R_{\text{NS}}^2 B_{\text{NS}} = R_*^2 B_* \quad (5.1)$$

or

$$B_{\text{NS}} = B_* \left(\frac{R_*}{R_{\text{NS}}} \right)^2 \quad (5.2)$$

with $R_* \sim 700000$ km, $R_{\text{NS}} = 10$ km and typical pre supernova stellar B -fields of $B_* \sim 100$ G, giving $B_{\text{NS}} = 5 \times 10^9 \times 10^2$ G = 5×10^{11} G.

Young Neutron Stars are expected to have magnetic fields on the order of 10^{12} G (10^8 T).

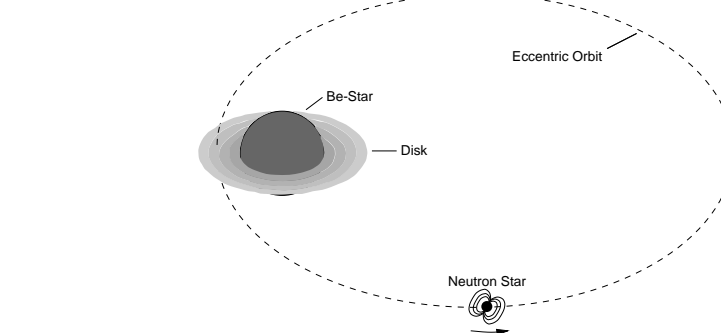
Theories in which neutron star magnetic fields are formed after the supernova yield similar results.

→ Will look at young neutron stars, i.e. High Mass X-ray Binaries.



5-4

Be Accretion

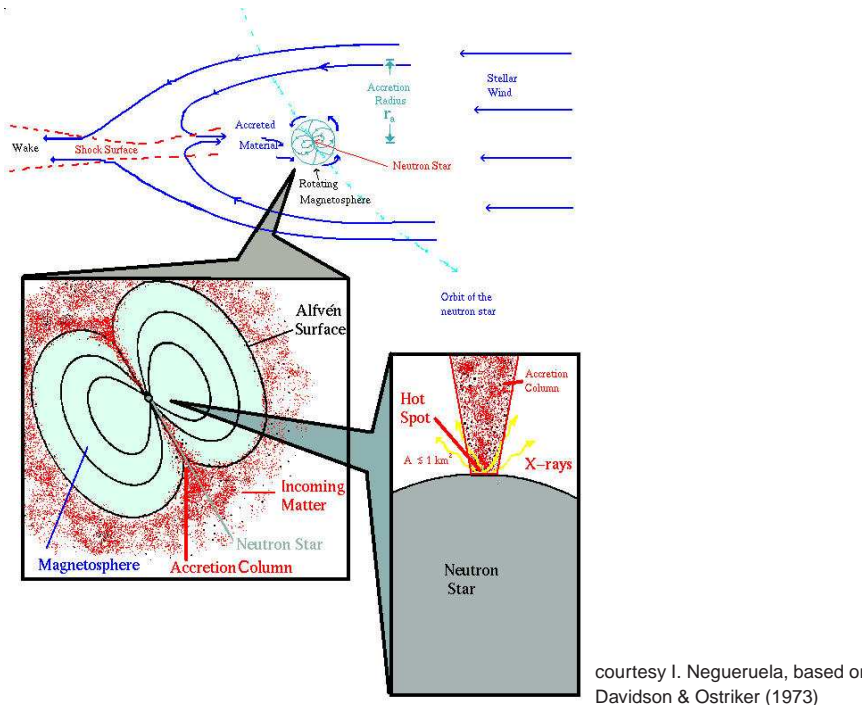


(Kretschmar 1996, Dissertation AIT, Abb. 2.6)

Some early type stars (O9-B2) have very high rotation rates ⇒ Formation of disk-like stellar wind at equator. Line emission from disk: Be phenomenon.

Collision of neutron star with disk results in irregular X-ray outbursts.

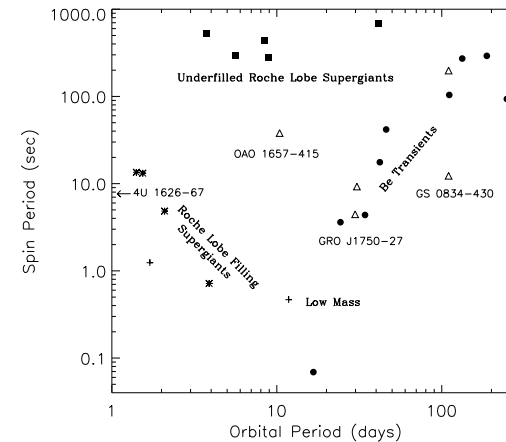
Example: A0535+26.



Torquing of the Disk

Corbet diagram: Spin period vs. orbital period for HMXB

- Roche lobe overflow: low P_{spin} , low P_{orb} , $L_X \gtrsim 10^{37} \text{ erg s}^{-1}$
- Wind accretors: longer orbital periods (to avoid Roche lobe overflow), $L_X \sim 10^{35-37} \text{ erg s}^{-1}$
- Be systems: correlation between spin and orbital periods (higher P_{orb} : less time to torque neutron star?).



High Mass X-ray Binaries

9



Torquing of the Disk

5-10

At distance r from the Neutron Star, the Keplerian velocity is

$$v = \sqrt{\frac{GM}{r}} \quad (5.3)$$

and therefore the orbital period ("Kepler period") and frequency are

$$P_K = \frac{2\pi r}{v} = \sqrt{\frac{4\pi^2 r^3}{GM}} \iff \Omega_K = \frac{2\pi}{P_K} = \sqrt{\frac{GM}{r^3}} \quad (5.4)$$

For $r = 1800 \text{ km}$ and $M = 1.4 M_\odot$, $P = 1 \text{ s}$.

Since the magnetic field couples the accretion disk to the neutron star, we expect accreting neutron stars to have periods on the order of one second.

... provided the coupling between the accretion disk and the B -field is strong enough



Torquing of the Disk

5-12

Coupling between magnetic field and accretion disk: accretion disk exerts torque onto NS:

$$I\dot{\omega} = \dot{M}r_{\text{mag}}^2\Omega_K(r_{\text{mag}}) = \dot{M}\sqrt{GMr_{\text{mag}}} \quad (5.5)$$

where the moment of inertia of the neutron star is $I = (2/5)MR_*^2$ and where $\Omega_K(r_{\text{mag}})$ is the Kepler frequency at r_{mag} (Eq. 5.4).

Derivation: disk angular momentum: $\mathcal{L} = rmv = r^2M\Omega$, and therefore the torque is $N = d\mathcal{L}/dt = r^2\dot{M}\Omega$, provided no feedback goes back into the disk.

The luminosity of the source is roughly given as

$$L = \frac{\dot{GMM}}{r_{\text{mag}}} \quad (5.6)$$

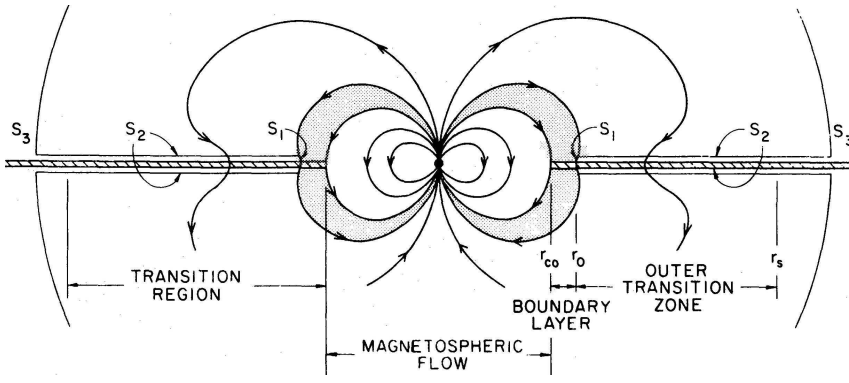
After some tedious algebra (Ghosh & Lamb, 1979), one obtains

$$-\frac{\dot{P}}{P} \propto P L^{6/7} \quad (5.7)$$



5-13

Torquing of the Disk



(Ghosh & Lamb, 1979)

In reality the magnetic field is perturbed by the accretion disk

⇒ calculations get messy

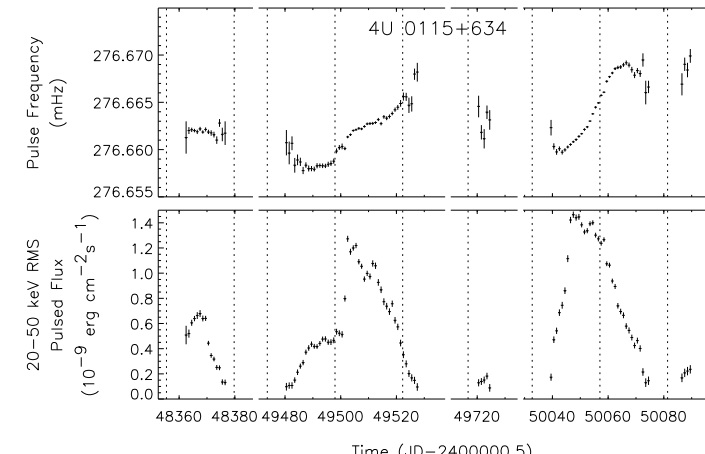
But we'll ignore this...

High Mass X-ray Binaries

11

5-15

Torquing of the Disk

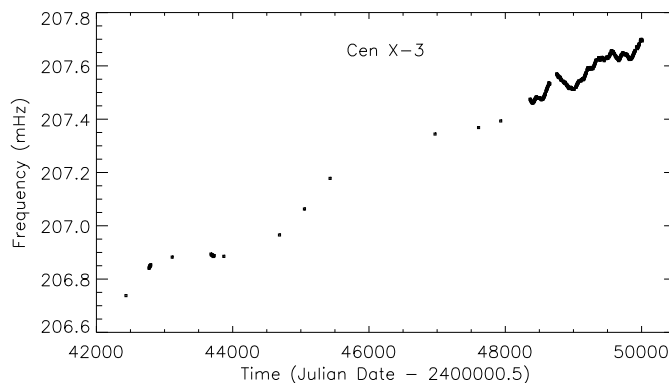


(Bildsten et al., 1997, 4U0115+63 is a Be system, dashed lines are periastron passages)

For transient systems, spin up is correlated with outbursts (i.e., increased \dot{M}).

5-14

Torquing of the Disk



(Bildsten et al., 1997)

Frequency behavior of the HMXB Cen X-3: long-term spin up trend

Spin up: Pulsar becomes faster (i.e., f goes up, resp. P goes down).Spin down: Pulsar becomes slower (i.e., f goes down, P goes up).

High Mass X-ray Binaries

12

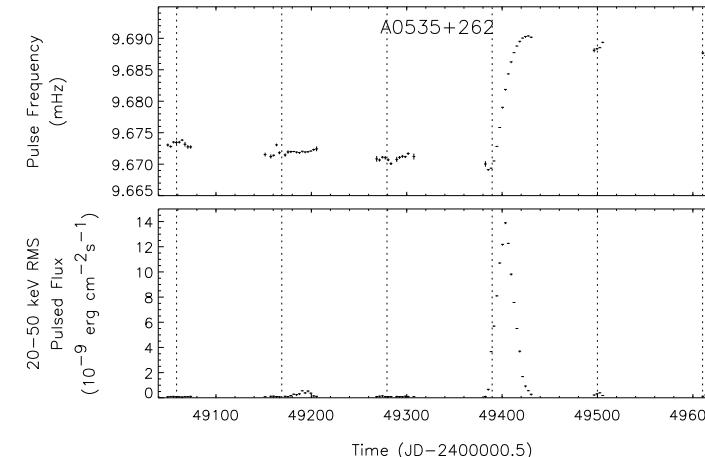
13

High Mass X-ray Binaries



5-16

Torquing of the Disk



(Bildsten et al., 1997)

For transient systems, spin up is correlated with outbursts (i.e., increased \dot{M}).

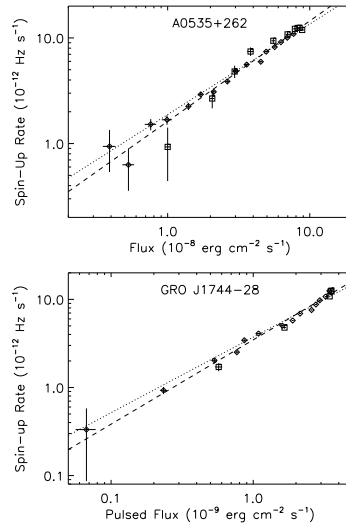
High Mass X-ray Binaries

14



5-17

Torquing of the Disk



Relationship between \dot{P} and F_X for outbursts of two Be systems.
Dotted: $\dot{P} \propto L^{6/7}$, dashed: best fit power law.
⇒ Individual outbursts follow torque theory!

more or less, perhaps due to difficulty in determining bolometric luminosity?

(Bildsten et al., 1997, Fig. 33)

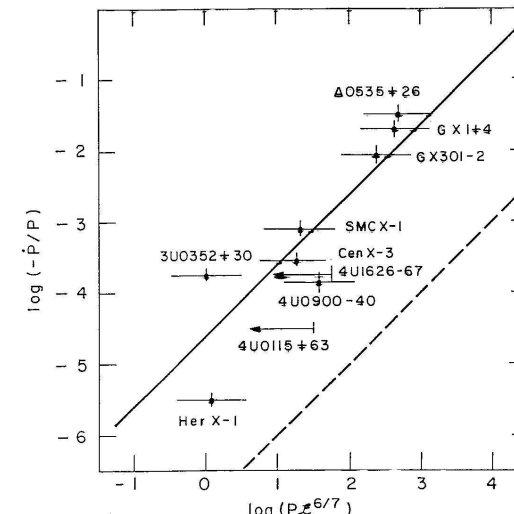
High Mass X-ray Binaries

15



5-19

Torquing of the Disk



Observations and prediction of magnetospheric accretion model seem to agree.

Note that this works *only* for the long-term trends and outbursts and that there is significant torque jitter superposed to these trends!

(Rappaport & Joss, 1977)

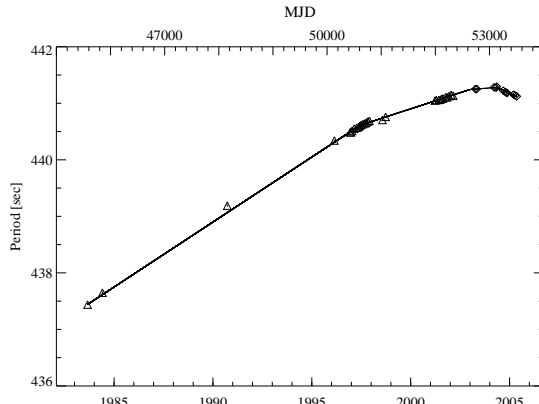
High Mass X-ray Binaries

17



5-18

Torquing of the Disk



(Fritz et al., 2006)

Not all systems show short term random walk behavior.
4U1907+09: longest continuous spin down in history.

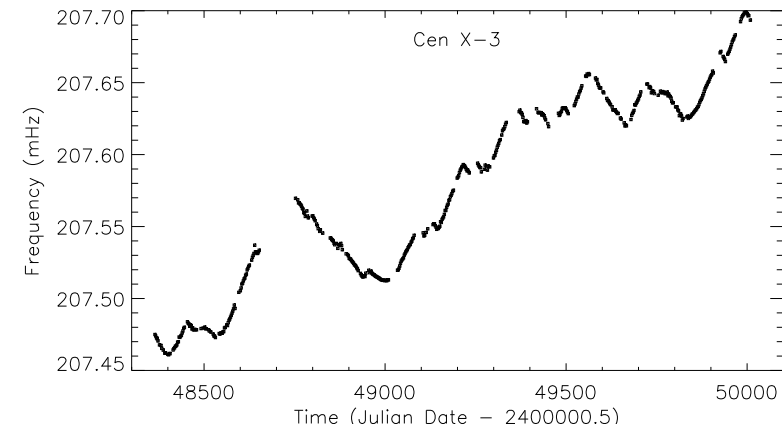
High Mass X-ray Binaries

16



5-20

Torquing of the Disk



(Bildsten et al., 1997)

Instantaneous torque behavior is very different from long term trends

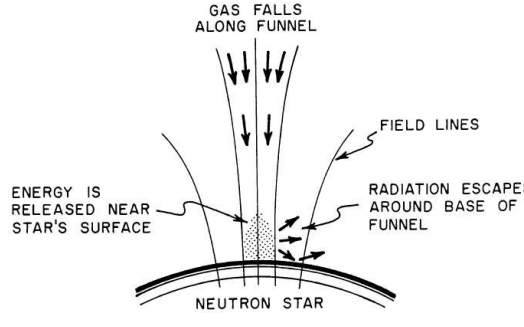
High Mass X-ray Binaries

18



5-21

The Neutron Star Poles: Basic Theory, I



Within R_{mag} , low density material
 \Rightarrow approximate free fall
 along B -field lines.
 Speed at magnetic pole:

$$v = \sqrt{\frac{2GM}{R}} \sim 0.65c$$

(~ 140 MeV nucleon $^{-1}$)

The area of the accreting spot is (for a dipolar B -field):

$$\pi r_0^2 = \pi R^2 \cdot (R/r_{\text{mag}}) \lesssim 1 \text{ km}^2$$

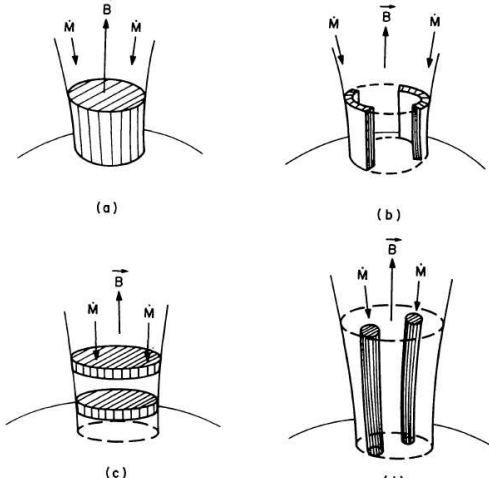
see also Pringle & Rees (1972), Gnedin & Sunyaev (1973), and Inoue (1975).

Accretion Column: Continuum Formation

1

5-22

The Neutron Star Poles: Basic Theory, II



Note: Whether accretion column is filled, a hollow funnel, or "spaghetti like" depends on the details of the coupling of the accretion disk to the B -field, which is not really understood.

(Mészáros, 1984, Fig. 11)

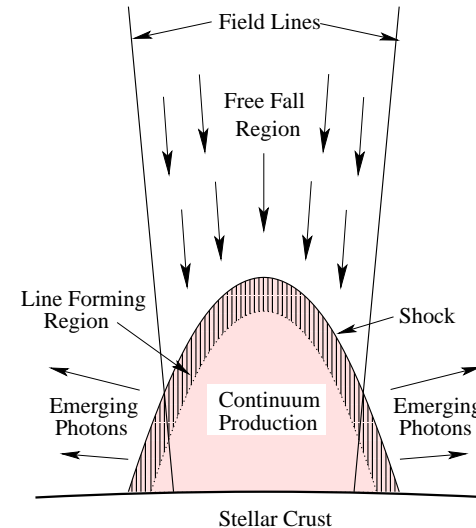
Accretion Column: Continuum Formation

2



5-23

The Neutron Star Poles: Basic Theory, III



Basic idea of continuum formation:

1. shock \Rightarrow low energy photons (bremsstrahlung)
2. Compton upscattering in accretion mound/column
3. Photons emerge once $\tau < 1$

Most important process modifying continuum: resonant Compton scattering

(Heindl et al., 2004)

Accretion Column: Continuum Formation

3



5-24

Landau Levels, I

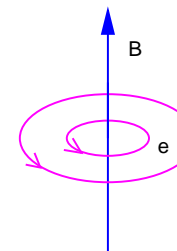
Strong field at neutron star's poles introduces exotic physics:

Quantization of electron energies $\perp B$ -field lines (Landau levels):

$$E_n = m_e c^2 \sqrt{\frac{1 + 2n(B/B_{\text{crit}}) \sin^2 \theta - 1}{\sin^2 \theta}}$$

p_{\parallel} : momentum of electron $\parallel B$ -field, n : major quantum number, B_{crit} is

$$B_{\text{crit}} = \frac{m_e^2 c^3}{e \hbar} \sim 4.4 \times 10^{13} \text{ G}$$



For $B \ll B_{\text{crit}}$, distance between Landau levels:

$$E_{\text{cyc}} = \frac{\hbar e}{m_e c} B = 11.6 \text{ keV} \left(\frac{B}{10^{12} \text{ G}} \right)$$

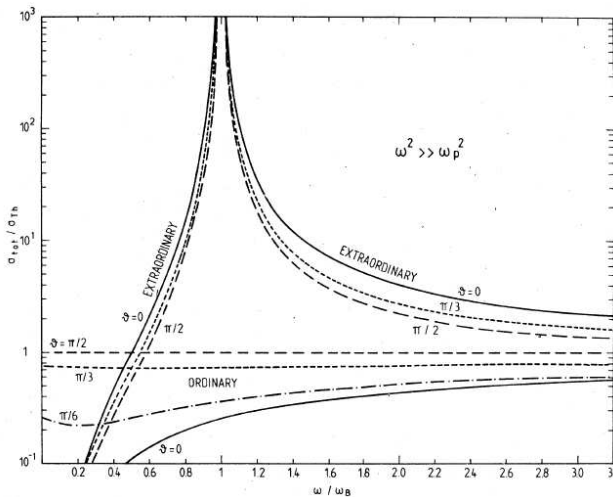
($12 - B_{12}$ -rule)
 \Rightarrow Cyclotron Resonance Scattering Features ("Cyclotron lines") at

$$E_n = n E_{\text{cyc}} = (1 + z) E_{n,\text{obs}}$$

($1 + z \sim 1.25 \dots 1.4$; grav. redshift!)

Accretion Column: Continuum Formation

4

**Landau Levels, II**

Radiation in accretion column interacts with resonant electrons
⇒ strong freq. dependence of the scattering cross section

Ventura (1979, Fig. 2), see Gonthier et al. (2000) for good approximations to the cross sections, and, e.g., Canuto (1970) and Canuto, Lodenquai & Ruderman (1971) for early work.

**Accretion Column, I**

Interaction of continuum radiation with electrons (Arons, Klein & Lea, 1987):
ordinary mode: E -field of photons in plane spanned by B -field and propagation direction. Continuum process only!

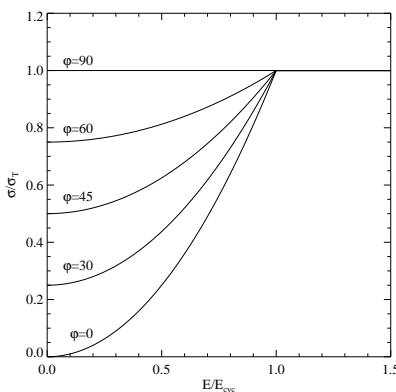
Cross section:

$$\sigma_{\text{ord}}(\varphi) = \sigma_T (\sin^2 \varphi + k(\epsilon) \cos^2 \varphi)$$

where

$$k(\epsilon) = \begin{cases} 1 & \text{for } E > E_{\text{cyc}} \\ (E/E_{\text{cyc}})^2 & \text{for } E \leq E_{\text{cyc}} \end{cases}$$

where $\sigma_T = 6.65 \times 10^{-25} \text{ cm}^2$ is the Thomson cross section, and where $\phi = \angle(B, \text{dir. propagation})$. (using notation of Becker & Wolff, 2007)

**Accretion Column, II**

extraordinary mode: E -field of photons perpendicular to plane spanned by B -field and direction of propagation.

Continuum and resonant scattering possible.

Cross section:

$$\sigma_{\text{ext}}(\varphi) = \sigma_T k(\epsilon) + \sigma_\ell \phi_\ell(E, E_{\text{cyc}}, \varphi)$$

where

- σ_ℓ : resonant cross section,

$$\sigma_\ell \sim 1.9 \times 10^4 \frac{\sigma_T}{B_{12}}$$

- $\phi_\ell(E, E_{\text{cyc}}, \varphi)$: line profile

(~ Gaussian if taking thermal broadening into account)

**Accretion Column, III**

Approximate cross sections outside of resonance:

Mode averaged cross section $\parallel B$ ($\varphi = 0^\circ$):

$$\sigma_{\parallel} = \frac{1}{2} (\sigma_{\text{ord}}(0^\circ) + \sigma_{\text{ext}}(0^\circ)) \sim \sigma_T \left(\frac{E}{E_{\text{cyc}}} \right)^2$$

Mode averaged cross section $\perp B$ ($\varphi = 90^\circ$):

$$\sigma_{\perp} = \frac{1}{2} (\sigma_{\text{ord}}(90^\circ) + \sigma_{\text{ext}}(90^\circ)) = \sigma_T + \sigma_T \left(\frac{E}{E_{\text{cyc}}} \right)^2 \sim \sigma_T$$

Plasma is much more transparent parallel to the B -field than perpendicular to the B -field!

For order of magnitude estimates, use mean energy of radiation field, $\langle E \rangle$, instead of E in above equations.

**Accretion Column, IV**

Basko & Sunyaev (1976): Radiation pressure becomes important once

$$L_X \sim L_{\text{crit}} = 2.72 \times 10^{37} \text{ erg s}^{-1} \frac{\sigma_T}{\sqrt{\sigma_{\perp}\sigma_{\parallel}}} \left(\frac{M}{M_{\odot}} \right) \left(\frac{r_0}{R} \right)$$

For $L_X \gtrsim L_{\text{crit}}$ flow is super-Eddington and radiation pressure \gg gas pressure.

\Rightarrow radiation pressure dominated shock

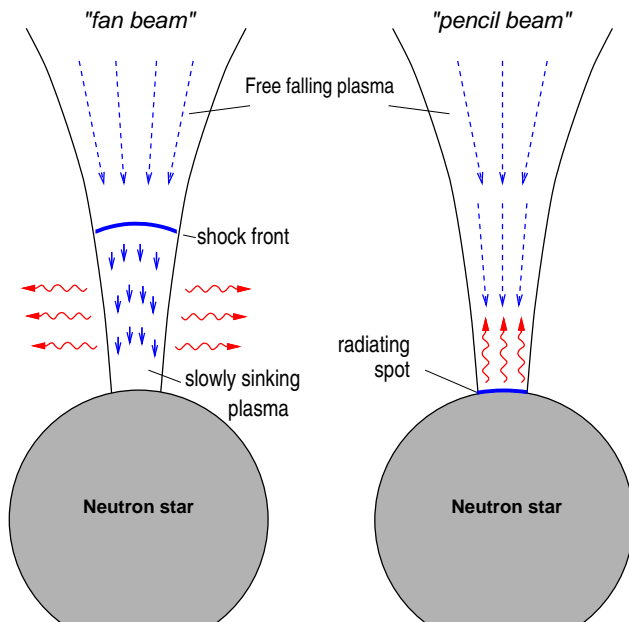
("accreted matter acts as test particles").

implies continuous velocity transition over few Thomson lengths, different from traditional hydrodynamical shocks!

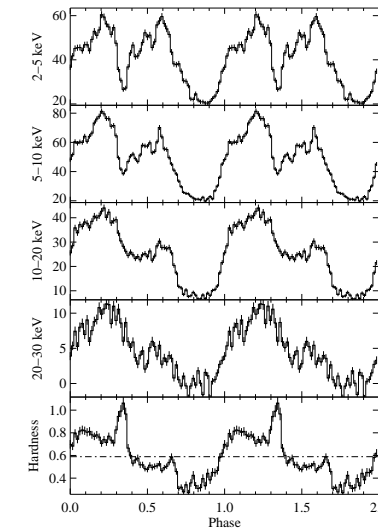
For $L_X \lesssim L_{\text{crit}}$: breaking of plasma by hydrodynamical shock, "Coulomb friction", or nuclear collisions (stopping length $\sim 30\text{--}60 \text{ g cm}^{-2}$).

see, e.g., Basko & Sunyaev (1976), Langer & Rappaport (1982), Braun & Yahel (1984)

What physical process is the most important is still very much debated.



(Kretschmar 1996, Dissertation AIT, Abb. 2.9 [after Harding 1994])
 \Rightarrow "cylinder" and "slab geometries"

**Pulse Profiles, I**

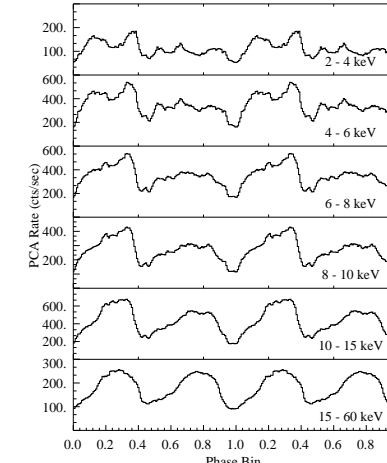
Rotation of accreting neutron star leads to X-ray pulsations.

Typically complex profiles at low E , \sim sinusoidal profiles at higher energies \Rightarrow due to emission characteristics and absorption in accretion flow?

Cep X-4 (McBride, et al., submitted)

Accretion Column: Continuum Formation

Accretion Column: Continuum Formation

**Pulse Profiles, II**

Rotation of accreting neutron star leads to X-ray pulsations.

Typically complex profiles at low E , \sim sinusoidal profiles at higher energies \Rightarrow due to emission characteristics and absorption in accretion flow?

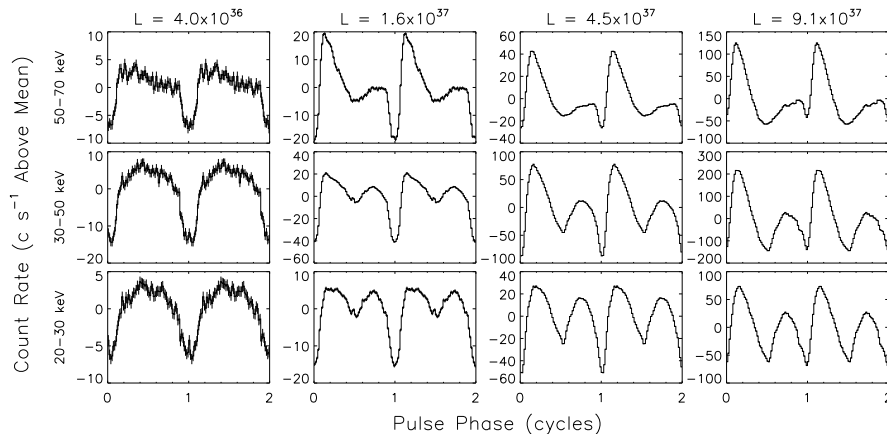
(Kreykenbohm et al., 1999, Vela X-1)

Accretion Column: Continuum Formation



5-33

Pulse Profiles, III



(Bildsten et al., 1997, A0535+35)

Luminosity dependence of the pulse profile of A0535+35 over one outburst.

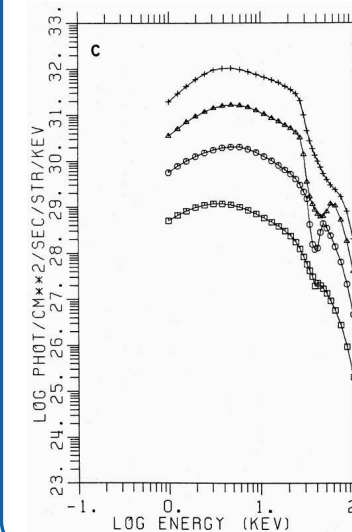
Accretion Column: Continuum Formation

13



5-35

Continuum Formation: Early Work



First simple models for accretion column by Nagel (1981a,b) used simplified radiative transfer (“two stream approximation”).

Mészáros & Nagel (1985a,b): angle dependent calculations based on Feautrier methods.

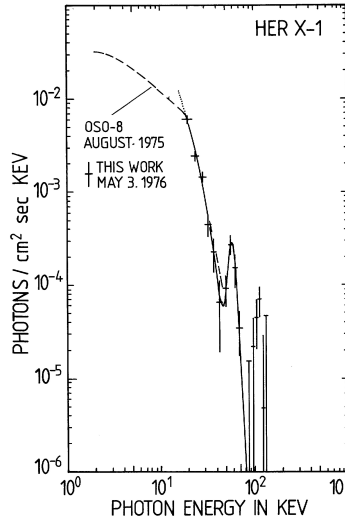
get continua \sim right (about one order of magnitude)

Spectra emerging from a slab (top to bottom $\theta = 21^\circ$, 48° , 71° , and 86° ; Mészáros & Nagel 1985a, Fig. 3c)



5-34

Spectral Shape



X-ray spectral shape:

- power law continuum with exponential cutoff
Due to Compton scattering?
- normally strong Fe K α line at 6.4...6.7 keV
Due to fluorescence in circumstellar material.
- Cyclotron line due to strong B -field

Her X-1 (Trümper et al., 1978)

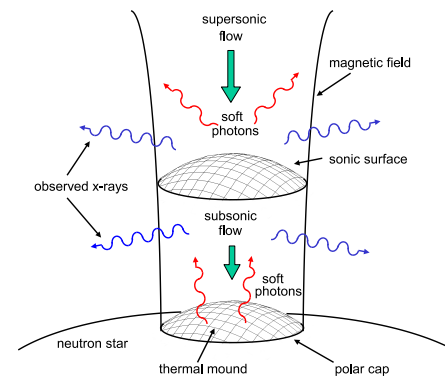
Accretion Column: Continuum Formation

14



5-36

Continuum Formation: State of the Art



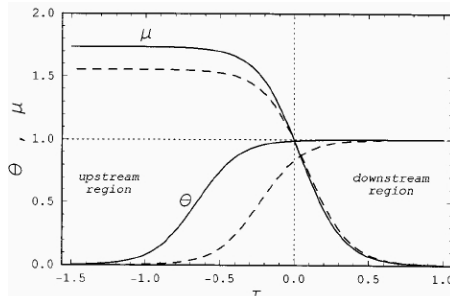
- Becker & Wolff (2005a,b, 2007): Previous work ignores accretion shock.
New picture: bulk motion Comptonization
- accretion mound produces soft X-rays
 - X-rays are upscattered in accretion shock
 - hard X-rays diffuse through walls of accretion column

Accretion Column: Continuum Formation

16



Continuum Formation: State of the Art



(Becker, 1998, Fig. 2)

- v_c : sonic point velocity,

$$v_c = \frac{4}{7} \left(\frac{2GM}{R} \right)^{1/2} \sim 0.37c$$

(for typical neutron star parameters)

Velocity structure of column (Becker, 1998):

$$\beta = \frac{v(x)}{v_c} = \frac{7}{4} \left(1 - \left(\frac{7}{3} \right)^{-1+x/x_{st}} \right)$$

where

- x : distance into column
- x_{st} : distance of sonic point from NS surface,

$$x_{st} = \frac{r_0}{2\sqrt{3}} \left(\frac{\sigma_\perp}{\sigma_\parallel} \right)^{1/2} \ln \left(\frac{7}{3} \right)$$

Continuum Formation: State of the Art

Mathematical implementation of the model: calculate Green's function, f_G , for response of column:

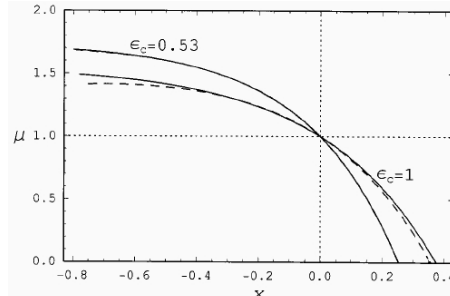
$$\begin{aligned} v \frac{\partial f_G}{\partial x} &= \frac{dv}{dx} \frac{\epsilon}{3} \frac{\partial f_G}{\partial \epsilon} && \text{bulk Comptonization (1st order Fermi)} \\ &+ \frac{\partial}{\partial x} \left(\frac{c}{3n_e \sigma_\parallel} \frac{\partial f_G}{\partial x} \right) && \text{spatial diffusion in } x\text{-direction (\parallel column axis)} \\ &- \frac{f_G}{t_{esc}} && \text{escape from the column} \\ &+ \frac{\dot{N}_0 \delta(\epsilon - \epsilon_0) \delta(x - x_0)}{\pi r_0^2 \epsilon_0^2} && \text{photon injection} \\ &- \beta v_0 f_G \delta(x - x_0) && \text{absorption in the thermal mound} \end{aligned}$$

where

- ϵ : photon energy
- n_e : electron number density
- $v_0 = v(x_0)$: flow velocity at source location x_0
- $\epsilon^2 f_0 d\epsilon$: photon number density at x_0
- β : absorptivity of the mound, determined self-consistently



Continuum Formation: State of the Art



(Becker, 1998, Fig. 9)

- v_c : sonic point velocity,

$$v_c = \frac{4}{7} \left(\frac{2GM}{R} \right)^{1/2} \sim 0.37c$$

(for typical neutron star parameters)

Velocity structure of column (Becker, 1998):

$$\beta = \frac{v(x)}{v_c} = \frac{7}{4} \left(1 - \left(\frac{7}{3} \right)^{-1+x/x_{st}} \right)$$

where

- x : distance into column
- x_{st} : distance of sonic point from NS surface,

$$x_{st} = \frac{r_0}{2\sqrt{3}} \left(\frac{\sigma_\perp}{\sigma_\parallel} \right)^{1/2} \ln \left(\frac{7}{3} \right)$$

Continuum Formation: State of the Art

Becker & Wolff (2005a,b): bulk Comptonization only (via Kompaneets equation, i.e., no Compton recoil)

\Rightarrow no cutoff, $\Gamma \geq 2$

This limitation has been removed by Becker & Wolff (2007).

Physical processes for scattering:

- bulk Comptonization
- thermal Comptonization

(via Kompaneets equation).

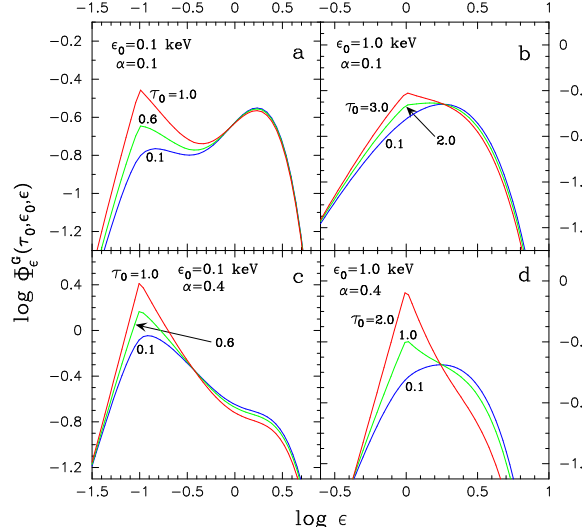
Seed photons:

- bremsstrahlung (from within column)
- cyclotron radiation (from within column)
- black body radiation (from bottom of column)



5-40

Continuum Formation: State of the Art



Column integrated
Green's functions as a
function of energy and
optical depth.
(assuming $\sigma_{\parallel} = 10^{-3} \sigma_T$,
 $\sigma_{\perp} = \sigma_T$).

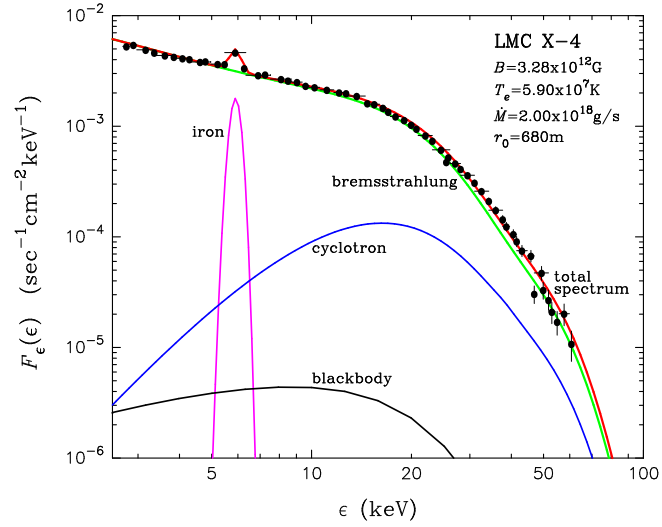
(Becker & Wolff, 2007, Fig. 3)

Accretion Column: Continuum Formation

21

5-42

Continuum Formation: State of the Art



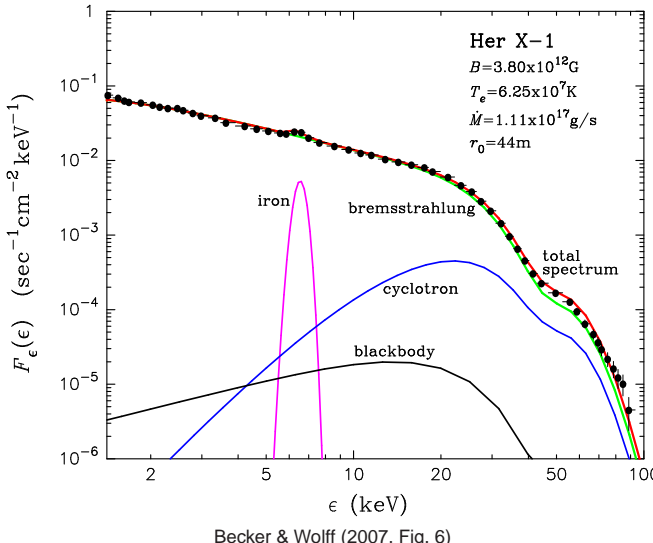
Becker & Wolff (2007, Fig. 7)

23



5-41

Continuum Formation: State of the Art



Becker & Wolff (2007, Fig. 6)

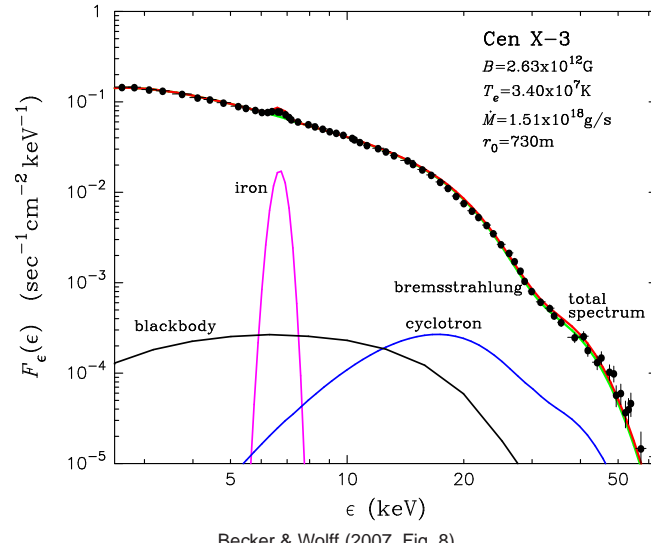
Accretion Column: Continuum Formation

22



5-43

Continuum Formation: State of the Art



Becker & Wolff (2007, Fig. 8)

24

Accretion Column: Continuum Formation